

# Spatiotemporal Analysis of COVID-19 Lockdown Impact on the Land Surface Temperatures of Different Land Cover Types in Louisiana

Priscilla M. Loh\*, Yaw A. Twumasi, Zhu H. Ning, Matilda Anokye, Diana B. Frimpong, Judith Oppong, Abena B. Asare-Ansah, Recheal N. D. Armah, Caroline Y. Apraku

Department of Urban Forestry, Environment and Natural Resources, Southern University and A&M College, Baton Rouge, USA  
Email: \*priscilla.loh@sus.edu, \*mawudonna@gmail.com

**How to cite this paper:** Loh, P.M., Twumasi, Y.A., Ning, Z.H., Anokye, M., Frimpong, D.B., Oppong, J., Asare-Ansah, A.B., Armah, R.N.D. and Apraku, C.Y. (2023) Spatiotemporal Analysis of COVID-19 Lockdown Impact on the Land Surface Temperatures of Different Land Cover Types in Louisiana. *Journal of Geographic Information System*, 15, 458-481.

<https://doi.org/10.4236/jgis.2023.155023>

**Received:** March 27, 2023

**Accepted:** October 6, 2023

**Published:** October 9, 2023

Copyright © 2023 by author(s) and Scientific Research Publishing Inc. This work is licensed under the Creative Commons Attribution International License (CC BY 4.0).

<http://creativecommons.org/licenses/by/4.0/>



Open Access

## Abstract

The COVID-19 pandemic posed a serious threat to life on the entire planet, necessitating the imposition of a lockdown mechanism that restricted people's movements to stop the disease's spread. This period experienced a decline in air pollution emissions and some environmental changes, offering a rare opportunity to understand the effects of fewer human activities on the earth's temperature. Hence, this study compares the changes in Land Surface Temperature (LST) that were observed prior to the pandemic (March & April 2019) and during the pandemic lockdown (March & April 2020) of three parishes in Louisiana. The data for this study was acquired using Landsat 8 Thermal Infrared Sensor (TIRS) Level 2, Collection 2, Tier 2 from the Google Earth Engine Catalog. For better visualization, the images that were derived had a cloud cover of less than 10%. Also, images for the three study areas were processed and categorized into four main classes: water, vegetation, built-up areas, and bare lands using a Random Forest Supervised Classification Algorithm. To improve the accuracy of the image classifications, three Normalized Difference Indices namely the Normalized Difference Vegetation Index (NDVI), Normalized Difference Water Index (NDWI) and Normalized Difference Built-Up Index (NDBI) were employed using the Near Infrared (NIR), Red, Green and SWIR bands for the calculations. After, these images were processed in Google Earth Engine to generate the LST products gridded at 30 m with a higher spatial resolution of 100 m according to the pre-pandemic (2019) and lockdown (2020) periods for the three study areas. Results of this study showed a decrease in LST values of the land cover classes from 2019 to 2020, with LST values in East Baton Parish decreasing from 44°C to 38°C, 42°C to 38°C in

Lafayette Parish, and 43°C to 38°C in Orleans Parish. The variations in the LST values therefore indicate the impact of fewer anthropogenic factors on the earth's temperature which requires regulatory and mitigative measures to continually reduce LST and control microclimate, especially in urban areas.

## Keywords

Urban Heat Island, Anthropogenic Activities, Greenhouse Gas, Greenspace, Wetlands

---

## 1. Introduction

Several concerns have been raised over the years regarding global warming and climate change of which most of the reasons are centered on the emission of harmful greenhouse gases resulting from anthropogenic factors. Commonly, urbanization, industrialization, the use of cars, aircraft, and other large-scale fossil fuel combustion activities are responsible for an increase in the production of greenhouse gases. Global warming, caused by heat trapping greenhouse gases (GHGs) such as Carbon Dioxide (CO<sub>2</sub>), Nitrous Oxide (N<sub>2</sub>O) or Methane (CH<sub>4</sub>) is considered the greatest environmental challenge in the 21st century causing an increase in Land Surface Temperature (LST), which is an average global air temperature near the surface of the Earth [1]. Land Surface Temperature is therefore considered a scale for measuring the surface Urban Heat Island (UHI) which [2] describes as resulting from the replacement of natural vegetation with low albedo building materials and roads especially in urban areas. According to the National Oceanic and Atmospheric Administration (NOAA), a portion of the energy that arrives from the sun is absorbed directly by the heat trapping gases released through human activities into the atmosphere whereas the other portion goes through the atmosphere to the surface of the earth, land or ocean [3], additionally posit that the earth is thought to be covered by these heat-trapping gases, acting as a blanket to retain heat near the surface and keep the globe "toastier". This means that the earth's surface gets hotter due to the greenhouse gases' concentration influencing how it would feel to touch in a particular location [4].

From a satellite's perspective, the surface is whatever it observes as it looks through the atmosphere to the ground, which could include buildings, bare lands, forests, water, or ice that are categorized as land cover types on the earth's surface [5]. Therefore, depending on the characteristics of the land surface and the activities that may increase or decrease surface warming, the land cover categories tend to influence varying surface temperatures. For instance, regions with more vegetation, ponds or waterbodies, experience cooling effects from evapotranspiration after absorbing the heat from solar radiation, which can assist in regulating the temperature [6] compared to more urbanized regions. Admittedly, in relation to land use and land cover types and their relationship with LST, the vegetation cover serves as a function of surface energy balance and a carbon

sink which is crucially linked to earth surface-atmosphere feedback mechanisms [7] For instance, in urbanized areas where the natural vegetation has typically been replaced by concrete and asphalt, the excess heat from buildings, transportation, industrialization, and residential areas is trapped causing the heat to accelerate to higher temperatures [6]. That is, the lower layer of the urban atmosphere's air temperature thereby modulates the land surface temperature, which is also a primary factor in the determination of the radiation from the surface and energy exchange [8]. To understand the phenomenon of LST variations, [8] also cited a study about the estimation of LST values in two cities in Ghana where the replacement of vegetation by asphalt and concrete for the construction of roads, buildings, and other structures contributes to the formation of UHI and impact on LST. An increase in UHI and consequently LST is driving the increased heat. The world is experiencing causing regional and seasonal temperature extremes, reduction in snow cover and sea ice, intensified heavy rainfall and changing habitat ranges for plants and animals [9].

Based on this, the Intergovernmental Panel on Climate Change (IPCC) suggests some pathways to limit warming to at least 1.5 degrees Celsius through the removal of carbon dioxide and other anthropogenic greenhouse gas emissions over the next decades [10] Also, [2] cited that there are several ways to counteract the negative impacts of UHI and enhance the internal natural ventilation of cities, including changing the way cities look and employing cool materials, enhancing green spaces and watering to lower the temperature of the surfaces as well as reducing greenhouse gas emissions. Reducing human activities, although seemingly impossible, is arguably one of the actions that can contribute to a reduction in the amount of greenhouse gas emissions and LST. By this, a worldwide pandemic presented a prospect where human activities came to a halt for a period of time. This pandemic known as the coronavirus disease (COVID-19) was detected in late 2019 and declared by the World Health Organization (WHO) as a pandemic and an infectious disease caused by the SARS-CoV-2 virus which could be spread from an infected person's mouth or nose in small liquid particles. To slow down the spread of COVID-19, strict measures were put in place by many governments around the world, referred to as a lockdown, aiming to reduce the frequency and duration of in-person interactions which drastically altered patterns of human activities [11]. Some of these measures implemented across the world included complete/partial travel bans, compulsory quarantines, market closures, lockdowns (only emergency services provided), social distancing and later vaccinations to control the spread of the pandemic.

In relation to reducing global warming, some researchers postulated how these initiated pandemic precautions to suspend human activities could have an impact on the land surface temperature and UHI due to a reduction in greenhouse gas emissions. Consequently, this also led to additional research being done to compare the land surface temperatures on various land covers, notably during pre-lockdown, lockdown, and post-lockdown phases. For instance, according to

[2] the research conducted to analyze land surface temperature in China's Yogyakarta city concluded in their research that a reduction in human activities decreased the effect of urban heat intensity and improved the environment and air quality. Although it is well known that Land Surface Temperature typically increases and decreases with impervious surface cover and vegetation cover, respectively, only a few city-wide studies have examined the impact of the presence and absence of human activities on Land Surface Temperature in Louisiana using geospatial data. Therefore, this study aims to fill a research gap relating to an absence of analysis on the changes in Land Surface Temperature observed during the COVID-19 lockdown period in Louisiana, particularly in three main areas Baton Rouge, Lafayette and Orleans. Referencing the statistics provided by [12], there have been variations in the three research locations' 12-month average temperature. For instance, the average temperature recorded in East Baton Rouge Parish was 69.2 degrees Fahrenheit between 2015 and 2018 which later decreased to 68.8 degrees Fahrenheit between 2018 and 2021 [12]. Similarly, Orleans Parish also experienced an average temperature decrease from 70.5 degrees Fahrenheit to 70 degrees Fahrenheit from 2015 to 2018 and 2018 to 2021 [12]. This decrease in average temperature was also recorded in Lafayette where the average temperature was 70 degrees Fahrenheit from 2015 to 2018 but decreased to 68.9 degrees Fahrenheit between 2018 and 2021 [12]. Based on the trend in temperature variations, the statistics indicate a significant drop in average temperature between December 2018 and November 2021 which coincides with the COVID-19 lockdown period (2020) where there were fewer human activities and a reduction in heat trapping gas emissions.

In light of this, this study therefore seeks to assess how the categories of land cover, namely, green spaces, bare lands, urbanized regions, and wetlands were impacted by land surface temperatures prior to and during the COVID-19 lockdown period. Specifically, using remote sensing data to examine pre-lockdown and lockdown effects, this assessment will be done in comparison with the changes in land surface temperature resulting from fewer human activities during the COVID-19 pandemic lockdown. To classify images from the three main study areas Baton Rouge, Lafayette, and New Orleans, the Normalized Difference Indices (NDIs), thus the Normalized Difference Vegetation Index (NDVI), Normalized Difference Built-Up Index (NDBI) and the Normalized Difference Water Index (NDWI) are employed respectively. According to [13], the NDVI, NDWI, and NDBI are all vegetation indices used in remote sensing to analyze different land features. That is, the NDVI is used to estimate vegetation density and productivity, the NDWI is used to estimate water content on earth, in plants and soil, whereas the NDBI is used to estimate the density of built-up areas, all on the earth's surface [13]. Also as cited by [14] the remote sensing indices, NDVI, NDWI, and NDBI help to extract areas of vegetation, water bodies, and built-up covers respectively. By assessing the effects of land surface temperature on different land cover types especially during the COVID lockdown period, the dynamics of the landscape under fluctuating surface temperature will inform proper maintenance de-

cisions by the authorities. The results will therefore add to the repository of knowledge concerning the impact of less human activities in the effect of COVID-19 lockdown on the different land cover types identified, as well as help in urban planning and proper land cover maintenance.

## 2. Research Methodology

### 2.1. The Study Areas

This study focused on three parishes located in Louisiana, one of the South-Central States which is geographically bound on the North by Arkansas, East by Mississippi, West by Texas, and South by the Gulf of Mexico [15]. The three study areas in Louisiana are categorized by land cover types according to Green Spaces, Wetlands and Urbanized areas in East Baton Rouge (EBR), New Orleans and Lafayette, respectively. These three study areas in Louisiana were selected due to their similarities in terms of industrialization activities and significant presence in the energy industry of the country. Baton Rouge is a home to several oil refineries and chemical plants and Lafayette has a strong oil and gas industry with New Orleans being a hub for offshore drilling and petroleum transportation. These industrial activities contribute to the emission of heat-trapping greenhouse gases that influence variations in LST.

#### 2.1.1. East Baton Rouge Parish

East Baton Rouge is one of the populous parishes in Louisiana which has the state's capital, Baton Rouge city. According to the [16] the East Baton Rouge Parish (**Figure 1**), recorded an estimated population of 453,301 people in 2021, with 220,553 people living in Baton Rouge. With this study area depicting green spaces, its vegetation has a tree cover in the city of Baton Rouge estimated at 44.6% [17]. The general climate is a humid subtropical climate with mild winters, hot and humid summers and moderate to heavy rainfall [18]. Due to the parish's position as a heartland of industrial activities in the Southeast, EBR has a long-standing history of air pollution issues and high temperatures [19].

#### 2.1.2. Orleans Parish

The Orleans Parish (**Figure 2**) is one of the study area parishes noted for its famous city, New Orleans. It is in the Mississippi River Delta, south of Lake Pontchartrain, on the banks of the Mississippi River Delta approximately 105 miles (169 km) upriver from the Gulf of Mexico. It has a subtropical climate, mild winters, as well as long, hot and humid summers, with frequent thunderstorms. Most parts of the Orleans parish are noted for being saturated or covered by water due to its proximity to the Gulf Mexico. Using the city, New Orleans as an example, the U.S. Census Bureau reports that the city's area is 350 square miles (910 km<sup>2</sup>), of which 169 square miles (440 km<sup>2</sup>) is land and 181 square miles (470 km<sup>2</sup>) (52%) is water [16]. This has made the city prone to water-related natural disasters such as hurricanes, flooding and storms which are considered to play a significant role in the parish's recent population dynamics. Thus, the parish recorded a



population of 376,971 in 2021 which is a -1.8 percent decline from the population estimated in 2020 at 383,997 [12].

### 2.1.3. Lafayette Parish

Lafayette Parish, one of the study areas in Louisiana, is part of Acadiana in Southern Louisiana, along the Gulf Coast (Figure 3). According to the [16] the parish has a total area of 269 square miles (700 km<sup>2</sup>), of which 269 square miles (700 km<sup>2</sup>) is land and 0.5 square miles (1.3 km<sup>2</sup>), that is 0.2 percent is covered by water. This indicates that the parish is made up of more developed, non-wetland areas, with Lafayette serving as its major municipality. Even though it is the fifth-smallest parish in Louisiana, the population of Lafayette Parish grew 9.7% from 222,513 people in 2010 to 244,205 in 2021 [12]. As far as temperature is concerned, the parish has witnessed a 1-degree Fahrenheit increase in its 12-month average temperature from November 1900 to October 2022. In the most recent month, October 2022, the average temperature in Lafayette Parish was 68 degrees Fahrenheit. This can be attributed to Lafayette still being the core of the oil and gas industry, with hundreds of related businesses in the parish and a highly skilled workforce [20].

### 2.2. Data Acquisition

Landsat 8 Thermal Infrared Sensor (TIRS) Level 2, Collection 2, Tier 2 data from

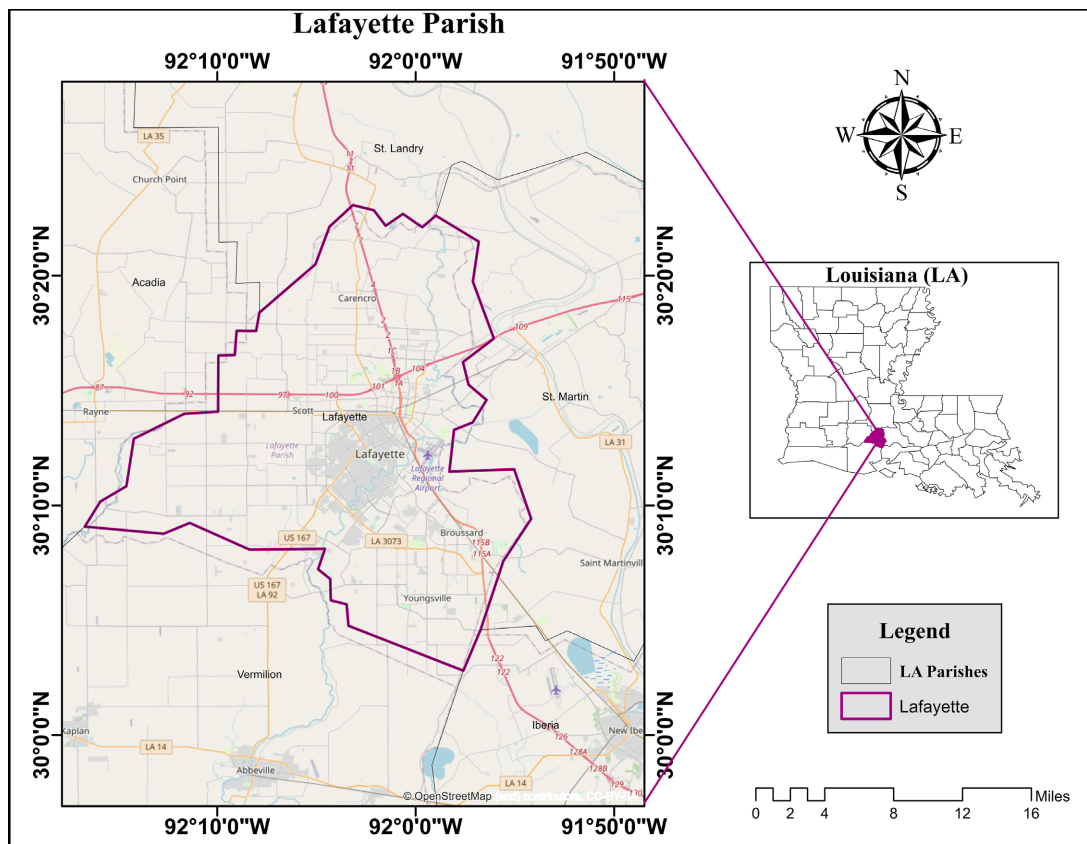


Figure 3. Location map of Lafayette Parish.

the Google Earth Engine Catalog were used for this study's data acquisition. The LST product is gridded at a resolution of 30 m, giving the data a spatial resolution of 100 m (or 328.08 feet). In terms of the images that were derived, this study used images with a cloud cover of less than 10% for clearer and better visualization. Also, the surface temperature band 10 or thermal band 10 was used for the calculations in this study mainly because it is recommended by the United States Geological Survey (USGS) as opposed to band 11 that has certain irregularities present. In order to calculate the Normalized Difference Indices for the classification of land use and land cover, bands 4, 5, 6, and 7 were employed. Since the study also concentrates on observations made prior to and during COVID-19 lockdown, the Landsat 8 imagery was collected for March and April from 2019 to 2020 respectively for the three regions of interest—Baton Rouge, New Orleans, and Lafayette. The spectral bands details of Landsat 8 OLI/TIRS are listed in **Table 1**.

### 2.3. Image Processing

This research work was implemented in Google Earth Engine (GEE). GEE enables effective geospatial studies by providing a robust cloud computing infrastructure and access to a large collection of petabytes of satellite imagery with the ability to do world scale analysis. GEE provides access and processing of data from public or their private catalogues to any user, thus accelerating scientific advancements. This platform was used to analyze and generate LST products with higher spatial resolution for the areas of interest based on Landsat 8 OLI/TIRS. The production chain was fully coded in JavaScript using the Code Editor Platform in GEE. The atmospherically corrected Landsat 8 Collection 2 Level 2 Surface Reflectance dataset (Landsat 8 SR) "LANDSAT/LC08/C02/T1\_L2" available in GEE, as provided by USGS was also used. The selection of the Collection 2 dataset was led by the fact that NASA cut off the supply chain for Collection 1 data and all the NASA

**Table 1.** Spectral band details of Landsat 8 OLI/TIRS.

Bands	Region in EM Spectrum	Wavelength	Resolution
Band 1	Visible (Coastal Aerosol)	430 - 450	30
Band 2	Visible (Blue)	450 - 510	30
Band 3	Visible (Green)	530 - 590	30
Band 4	Visible (Red)	640 - 670	30
Band 5	Near-Infrared (NIR)	850 - 880	30
Band 6	Short Wave-Infrared 1 (SWIR 1)	1570 - 1650	30
Band 7	Short Wave-Infrared 2 (SWIR 2)	2110 - 2290	30
Band 8	Panchromatic (PAN)	500 - 680	15
Band 9	Cirrus	1360 - 1380	30
Band 10	Thermal Infrared (TIRS1)	1060 - 1119	100
Band 11	Thermal Infrared (TIRS2)	1150 - 1251	100



data were reprocessed to Collection 2. This Landsat 8 collection derived from the Level 2 product was atmospherically corrected and hence required no preprocessing.

## 2.4. Land Cover Classification

A random forest supervised classification algorithm was employed to classify the three study areas into a total of four main classes thus, water, vegetation and built-up areas and bare land. Three Normalized Difference Indices including Normalized Difference Vegetation Index (NDVI), Normalized Difference Water Index (NDWI) and Normalized Difference Built-Up Index (NDBI) were employed to improve the accuracy of the image classifications. The remote sensing indices (NDVI, NDWI, and NDBI) were used in this study, and the same was extracted from the various bands of LANDSAT 8 (OLI & TIRS) satellite image using their standard formula. The Near Infrared (NIR), Red, Green and SWIR bands of the LANDSAT 8 image were used to calculate the Normalized Difference Indices in Google Earth Engine.

### 2.4.1. Accuracy Assessment

Based on retrieved land cover classes and the validation points, confusion matrices were calculated to determine the user, producer, and overall accuracy of the final land cover maps. Using the approach of Foody, the current research randomly validated 1500 points for the three different study sites. These sites have diverse landscape characteristics. The visual checking of each land cover classification was conducted using a Google Earth map for each site. A total of 500 points (pixels) was sampled via the stratified random approach for each study area.

### 2.4.2. Spectral Transformation of Landsat 8 OLI/TIRS Imagery

The vegetation density value was determined by Normalized Difference Vegetation Index (NDVI) with its formula.

$$\text{NDVI} = \frac{\text{NIR Band} - \text{Red Band}}{\text{NIR Band} + \text{Red Band}} \quad [8] [21] \quad (1)$$

NDWI was used to classify water bodies, and the water index was extracted by the given formula:

$$\text{NDWI} = \frac{\text{Green Band} - \text{NIR Band}}{\text{Green Band} + \text{NIR Band}} \quad [22] \quad (2)$$

Built-up area detection was done with Normalized Difference Built-Up Index (NDBI) using,

$$\text{NDBI} = \frac{\text{SWIR} - \text{NIR}}{\text{SWIR} + \text{NIR}} \quad [23] \quad (3)$$

## 2.5. Land Surface Temperature Analysis

Landsat thermal infrared measurements were utilized to estimate LST using the

single-channel (SC) method. Using Google Earth Engine, the following equations were used to calculate the Land Surface Temperature. From Landsat 8 OLI/TIRS given by the USGS and included in the GEE data catalog, Digital Numbers (DN) were converted to Top of Atmospheric radiance (TOA) using the formula:

$$\text{TOA} = M_L + Q_{CAL} + A_L \quad [8] [24] \quad (4)$$

where  $M_L$  = Multiplicative rescaling factor of band 10,  $Q_{cal}$  = Band 10,  $A_L$  = Additive rescaling factor of band 10.

To calculate brightness temperature, TOA and two thermal conversion constants were used as by the formula:

$$\text{Brightness Temperature (BT)} = \frac{K_2}{\ln \frac{K_1}{\text{TOA}} + 1} - 273.15 \quad [8] [24] \quad (5)$$

where  $K_1$  = Thermal conversion constant one of band 10,  $K_2$  = Thermal conversion constant two of band 10.

NDVI is used to calculate emissivity. NDVI and proportion (fractional) of vegetation are calculated using the formula:

$$\text{Proportion of Vegetation (P}_v\text{)} = \left( \frac{\text{NDVI} - \text{NDVI}_{\min}}{\text{NDVI}_{\max} - \text{NDVI}_{\min}} \right)^2 \quad [8] [24] \quad (6)$$

According to [8], emissivity is the radiation capacity of a surface compared to that of a black body. It is calculated by using the formula;

$$\text{Emissivity } (\varepsilon) = 0.004 * P_v + 0.986 \quad [25] \quad (7)$$

Finally, LST is calculated using equation 8 stated by:

$$\text{LST} = \frac{\text{BT}}{1 + \left( 0.0015 * \frac{\text{BT}}{1.4388} \right) * \ln \varepsilon} \quad [8] \quad (8)$$

### 3. Results and Discussion

This section is presented in three parts: 1) the results of Land Use and Land Cover and its relation to the spectral indices generated before and during the COVID Lockdown; 2) the results of Land Surface Temperature for the three study areas; and 3) an examination of the Land Surface temperature retrieved from the classes for each site to establish the relationship between LULC, and LST. All these parameters are assessed before and during the COVID-19 Lockdown in Louisiana.

#### 3.1. Land Cover and Spectral Indices

The values of NDVI vary from  $-1$  to  $+1$  whereby a higher NDVI value indicates the rich and healthier vegetative cover and vice versa. The resultant minimum and maximum NDVI values ranged from  $0.99$  to  $-1.03$  in East Baton Rouge,  $0.98$  to  $-0.928$  in East Lafayette and  $0.92$  to  $-0.72$  in East Orleans. East Baton Rouge is noted to have recorded the highest NDVI signifying a lot of vegeta-

tion cover. For the NDBI, the values of vary from  $-1$  to  $+1$  by which the NDBI values indicate increased developed or built ups (impervious surfaces). The resultant minimum and maximum NDBI values for this study however, ranged from 0.584 to  $-1.583$  for East Baton Rouge, 0.784 to  $-0.932$  for East Lafayette and 0.525 to  $-1.01681$  for East Orleans. Evidently, the NDBI is recorded highest for Lafayette indicating a landscape of extensive built-up areas. NDWI was calculated in this study to extract the water bodies of the three study areas. The resultant minimum and maximum NDWI values ranged from 1.0227 to  $-0.85$  for East Baton Rouge, 0.943 to  $-0.88$  for East Lafayette and 0.753 to  $-0.846$  for East Orleans. **Figures 4-6** show the NDVI, NDBI and NDWI maps (images) of the three study areas. These spectral indices were also added as bands to the Landsat 8 image to improve the accuracy of the Random Forest Land over Classification.

The results of the overall accuracy assessments of the final land cover maps are shown in **Table 2** below.

**Table 2.** Accuracy assessment results.

Land Cover Classes	East Baton Rouge		Lafayette		New Orleans	
	User Accuracy (%)	Error of Commission (%)	User Accuracy (%)	Error of Commission (%)	User Accuracy (%)	Error of Commission (%)
Water	93.33	6.667	82	18	100	0
Vegetation	86.67	13.333	67	33	100	0
Built-up	75.79	26.667	82	18	94	0
Bare land	73.33	24.210	76	24	92	8
<b>Overall Accuracy</b>	96		92		94	
<b>Kappa Statistic</b>	94		91		90	

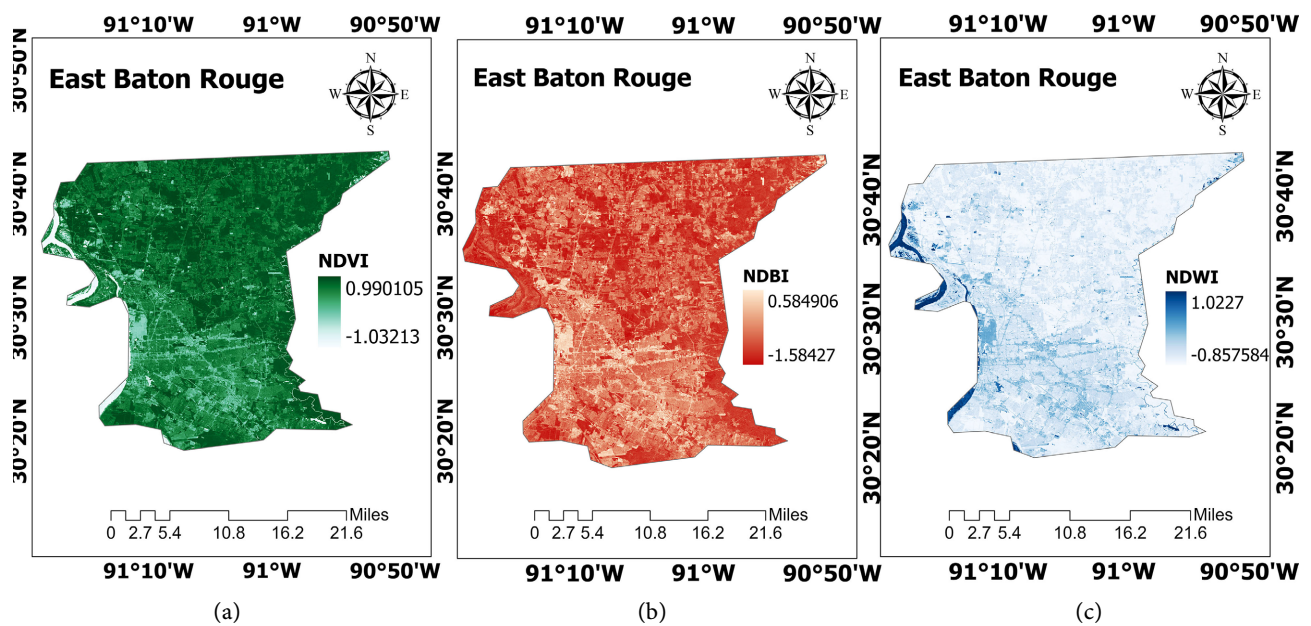


**Figure 4.** Spectral indices maps for East Baton Rouge: (a) NDVI; (b) NDBI; (c) NDWI.

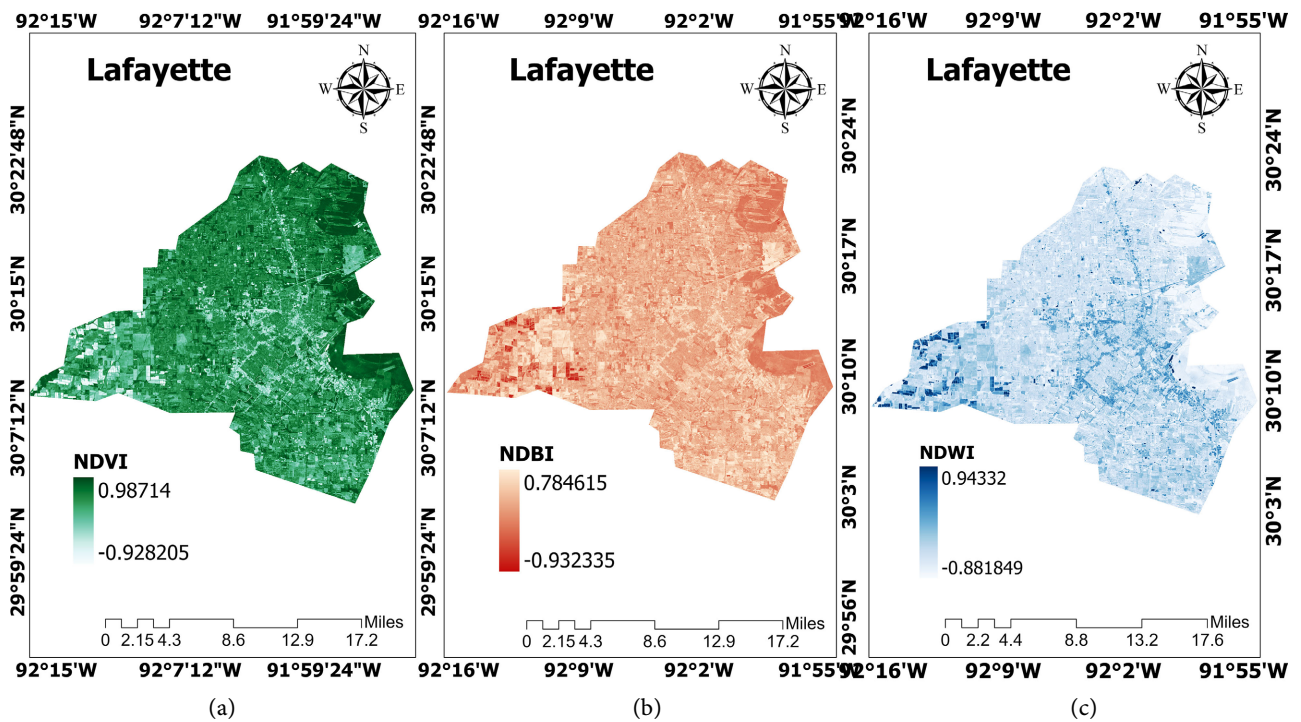


Figure 5. Spectral indices maps for East Lafayette: (a) NDVI; (b) NDBI; (c) NDWI.

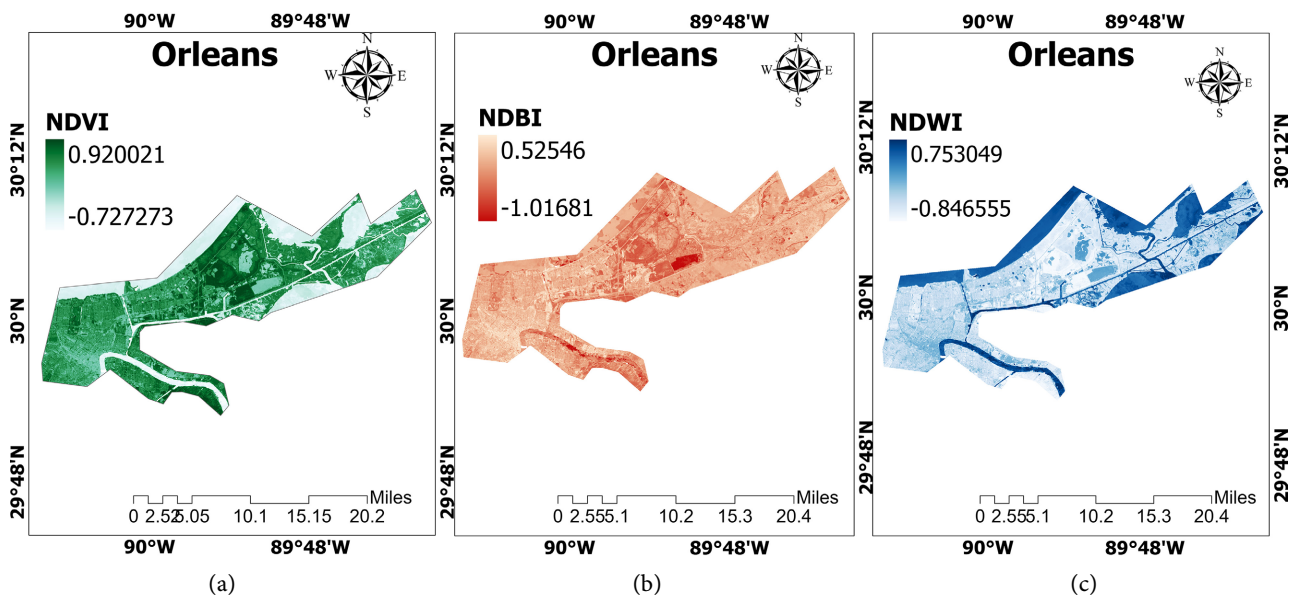
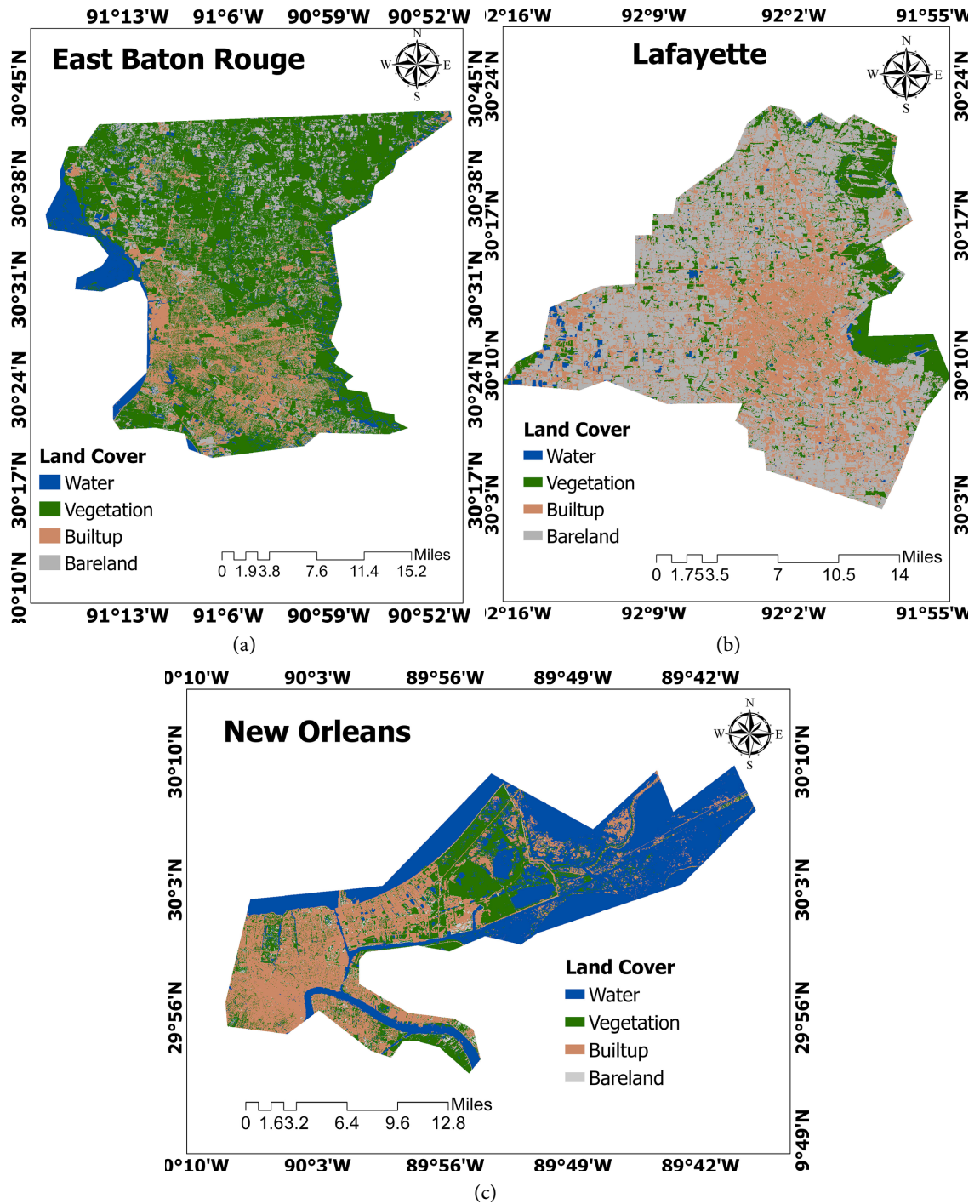


Figure 6. Spectral indices maps for East Orleans: (a) NDVI; (b) NDBI; (c) NDWI.

Four major LULC classes were identified in the current study area viz: 1) water, 2) vegetation, 3) built-up, 4) bare land. East Baton Parish indicates the parish has a high vegetation cover (Figure 7(a)) while Lafayette Parish indicates a high cover of built-up areas (Figure 7(b)), and Orleans Parish indicates a high cover of both water and built-up cover (Figure 7(c)). Overall, the LULC dynamics did not indicate a notable increment in the classes. Thus, one land cover map was used as a basis for the extraction of the LST values.



**Figure 7.** Land cover maps for: (a) East Baton Rouge; (b) East Lafayette (c) East Orleans.

### 3.2. Land Surface Temperature Analysis

Similar to the research conducted by [26] in the detection of land cover change and LST, a pixel to pixel-based extraction of land surface temperature was done for East Baton Rouge, East Lafayette, and East Orleans parishes. The distribution plots of land surface temperature for the corresponding land covers have been plotted in **Figures 8-13**. An attempt has been made to capture the changes and

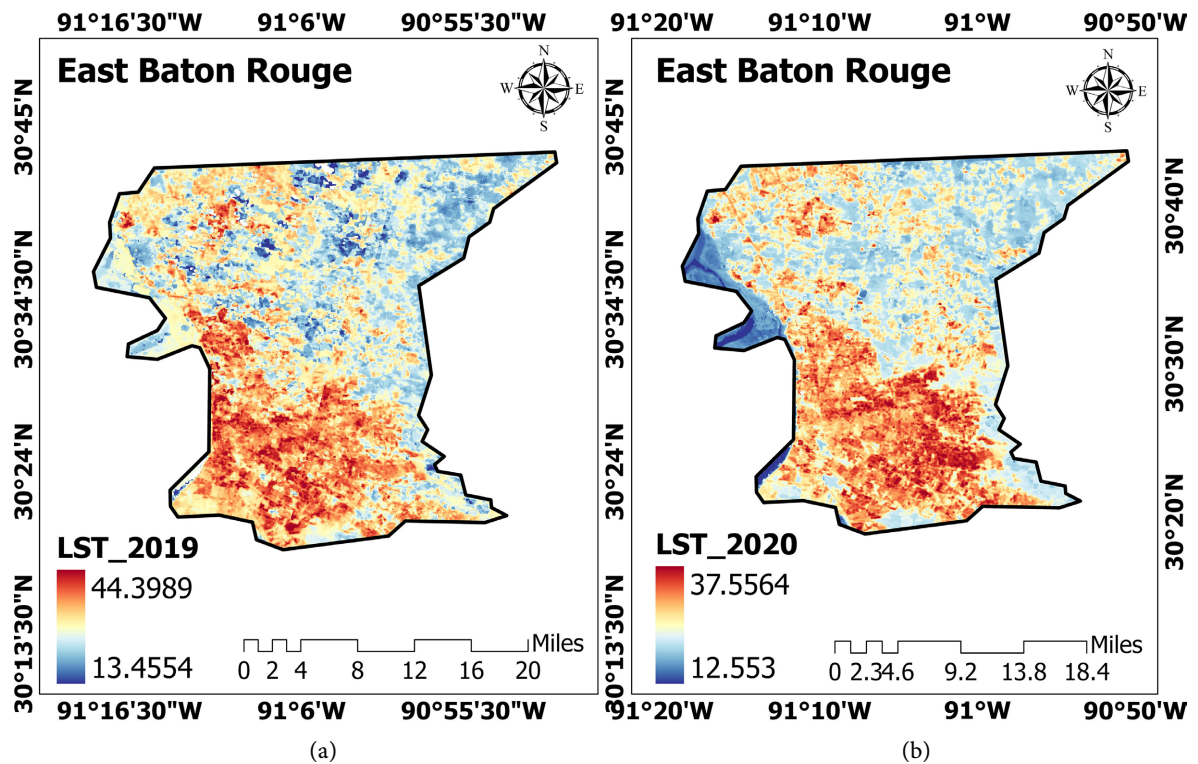
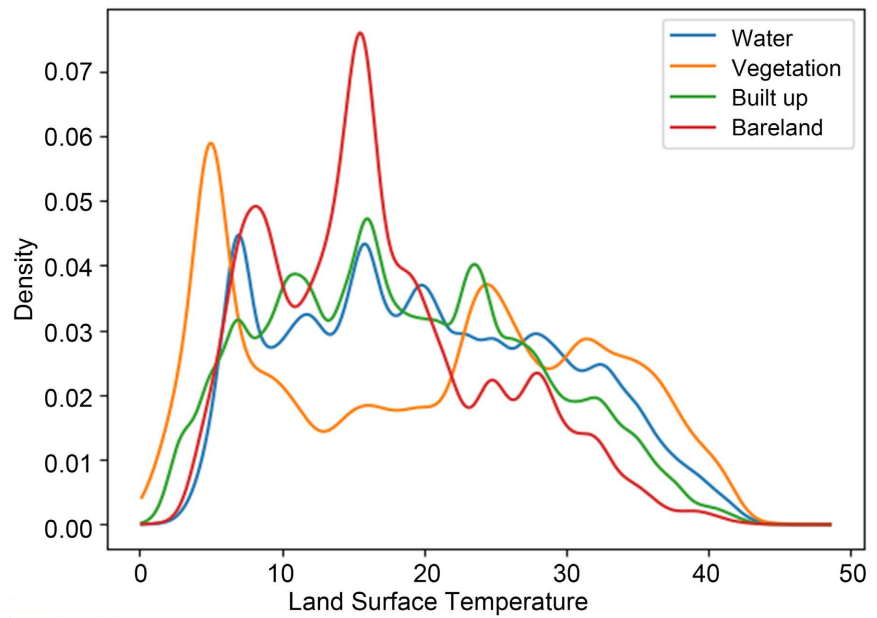
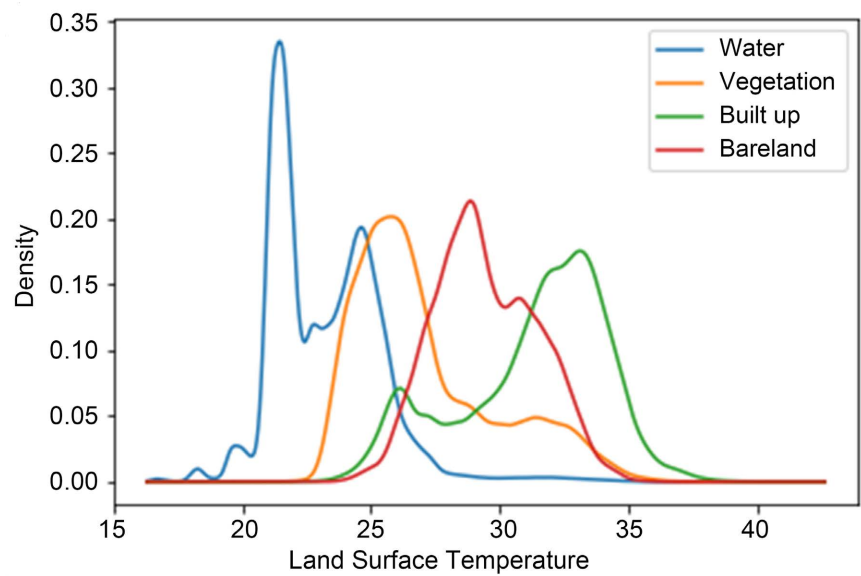


**Figure 8.** LST map for East Baton Rouge.

the effect of lockdown on these various land covers and their surface temperature. The lockdown across Louisiana was in effect from March to April 2020 during which movement restrictions were implemented across all parishes. Landsat imagery before the pandemic and during the lockdown has been collected for the respective locations mentioned above, and the land surface temperature has been extracted. LULC types that have been used for the study are built-ups, vegetation, water, and bare lands. In addition, to compare the changes that have occurred, the distribution curves for the years 2019 and 2020 are plotted for the months of March and April in each year. These distribution curves also reflect the land surface temperature that was recorded over each LULC before and during COVID-19. This was extracted to specifically examine the variations of reduction in the LST values that were recorded from the LULC in the three study areas during this period. Generally, from all the study areas, the distribution curves showed that there were significant reductions in the LST values during the COVID-19 lockdown period especially for vegetation areas and water bodies. That is, higher densities of these parameters were recorded during the lockdown period which could be traced to reduced LST values. LST is heavily influenced by air surface temperature, although it is a good indicator of heat-retaining or heat-reflecting surfaces. Built-up and urban regions have greater temperatures because they reflect more heat than the Earth's surface. This is due to the fact that most built-up regions comprise impermeable surfaces, such as buildings, which may absorb solar energy or radiation and release it back into the atmosphere to generate heat waves.



(a)



(b)

**Figure 9.** Land surface temperature distribution for various land covers in East Baton Rouge within the study period: (a) March 2019 (before lockdown) (b) March 2020 (during lockdown).

### 3.2.1. East Baton Rouge Parish

According to **Figure 8**, the LST difference for the period of the study in the area ranges from 44°C (before COVID-19) to 38°C (during the COVID-19 lockdown). The north-eastern part of the area shows relatively low temperature due to higher vegetation and reserve forest as in the NDVI and land cover maps of **Figure 5(a)** and **Figure 7(a)**. This is also reflected in **Figure 9** as all the land covers recorded lower LST values with higher density values particularly in waterbodies and vegetation.

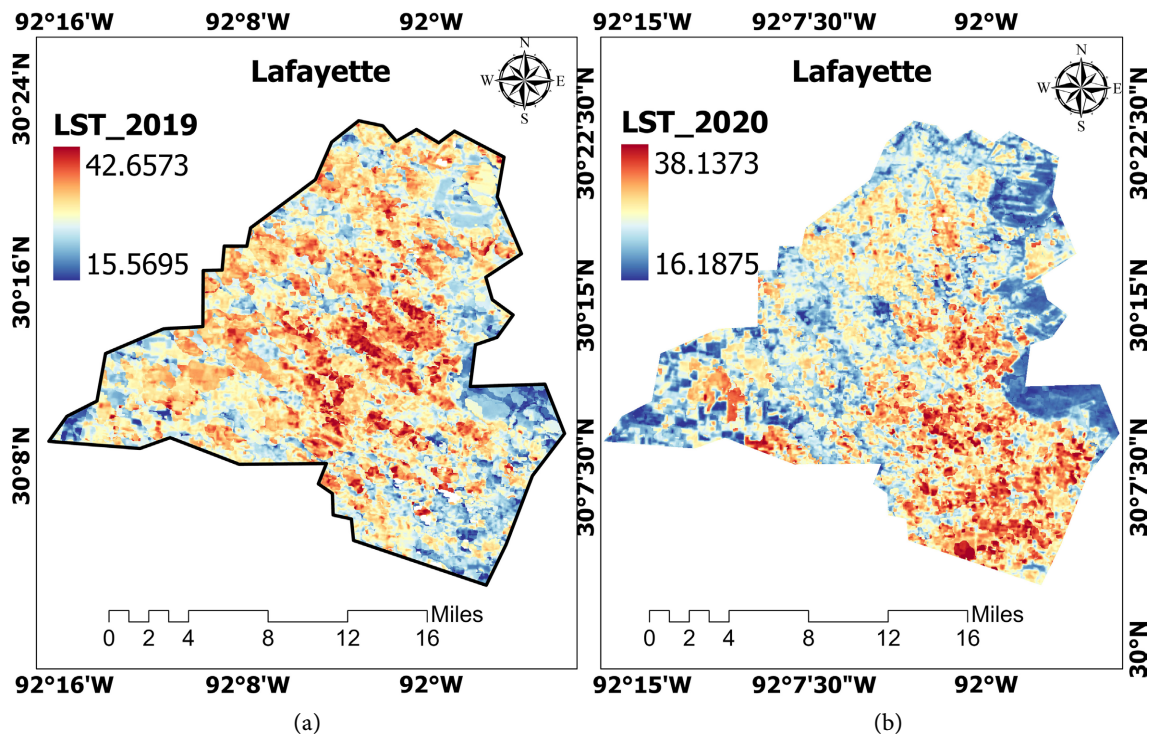


**Figure 10.** LST map for East Lafayette. (a) March 2019; (b) March 2020.

### 3.2.2. Lafayette Parish

**Figure 10** shows that the land surface temperature for Lafayette has decreased during the lockdown for the year 2020 compared to 2019. For the land cover of built ups, there was a decrease in temperature of  $4.34^{\circ}\text{C}$ . Next, barren land showed a reduction of  $4.58^{\circ}\text{C}$ . Water surfaces showed a reduction of  $2.21^{\circ}\text{C}$ . Vegetation showed a decrease of  $5.53^{\circ}\text{C}$  respectively. Evidently, the LST moved from approximately 43 degrees Celsius prior to the COVID-19 lockdown period to approximately 38 degrees Celsius during the lockdown period. That is, most of the built-up areas found within central Lafayette spreading across the north and central west recorded lesser LST values during the COVID-19 period and lockdown.

The effect of lockdown is visible for the Lafayette study location. With industries on lockdown and a decrease in the number of vehicles on the road during the period, the land surface temperature decreased. **Figure 11(b)** shows a distribution curve skewed to the right as the LST values decreased with higher density of vegetation and water for instance, and vice versa.

### 3.2.3. East Orleans Parish

The urban areas in East Orleans seemed to have higher temperatures than the other land cover types mostly covered by water, although this difference was less noticeable for the estimates from 28th July 2018. For instance, areas classified as water bodies, vegetation or green urban areas seemed, by means of visual analysis, to have the lowest temperatures while the areas with higher building density had higher temperatures.



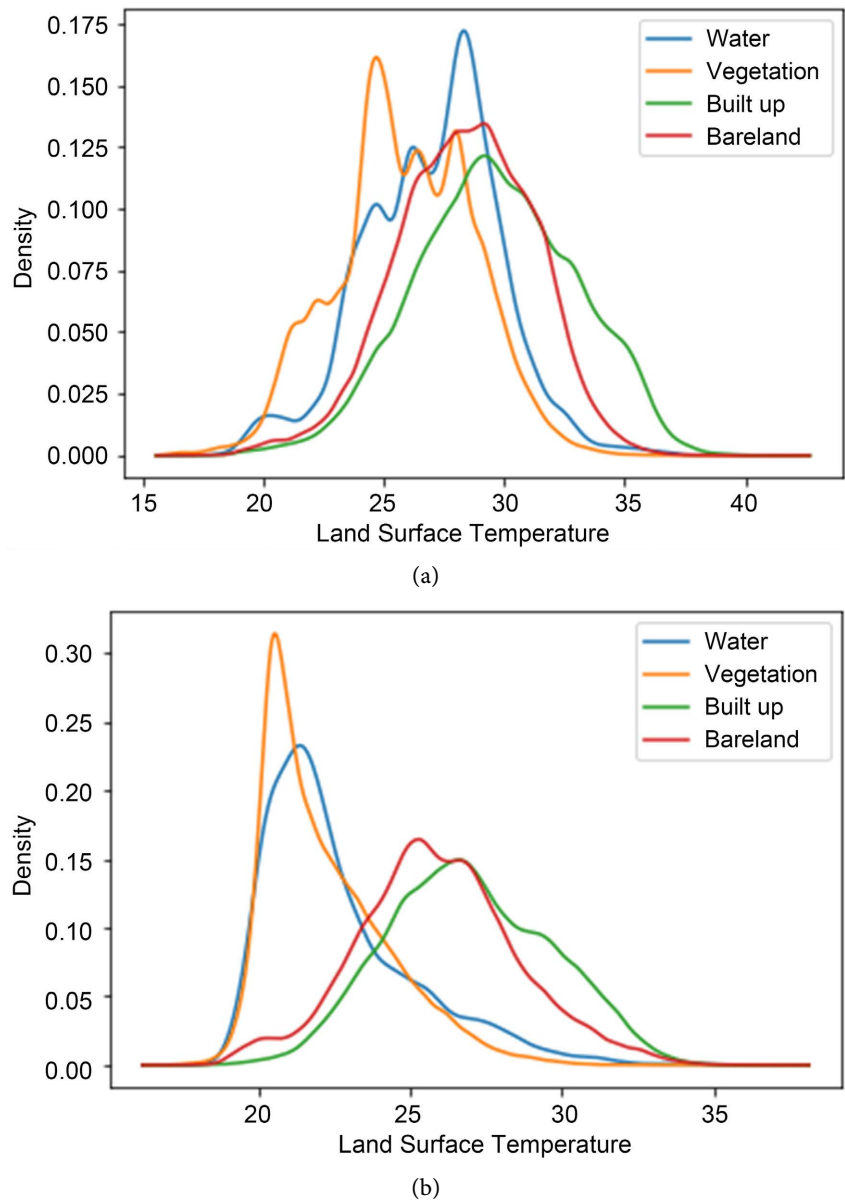


**Figure 11.** Land surface temperature distribution for various land covers in Lafayette within the study period: (a) March 2019 (before lockdown) (b) March 2020 (during lockdown).

The results (**Figure 12** and **Figure 13**) for the parish of Orleans are noticeable compared to the other two cities. There has been a significant decrease in temperature for the month of March 2020 (during lockdown) compared to March 2019. Buildings, barren land, vegetation, and water have shown a decrease in temperature of 5°C, 3.65°C, 4.01°C, and 4.08°C, respectively. Even though the impact of climate change has not been incorporated or studied in this work, one of the possible reasons for an observable change in the surface temperature is that the effect of lockdown might have been mitigated by climate change [2]. This is a possible indication that the lockdown rules were appropriately followed in Orleans.

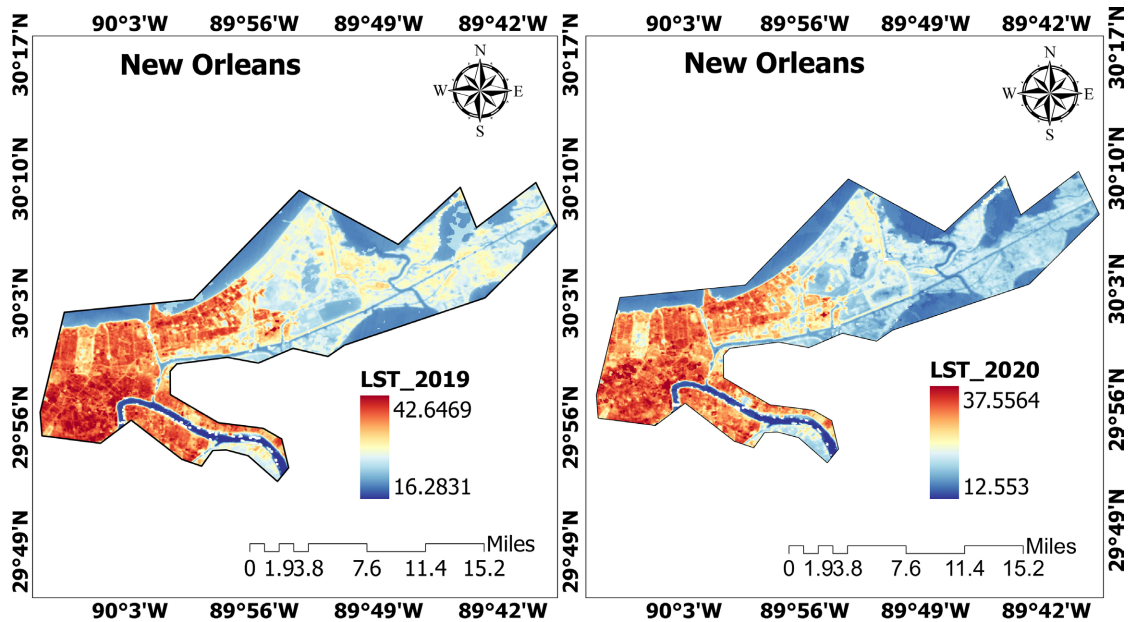
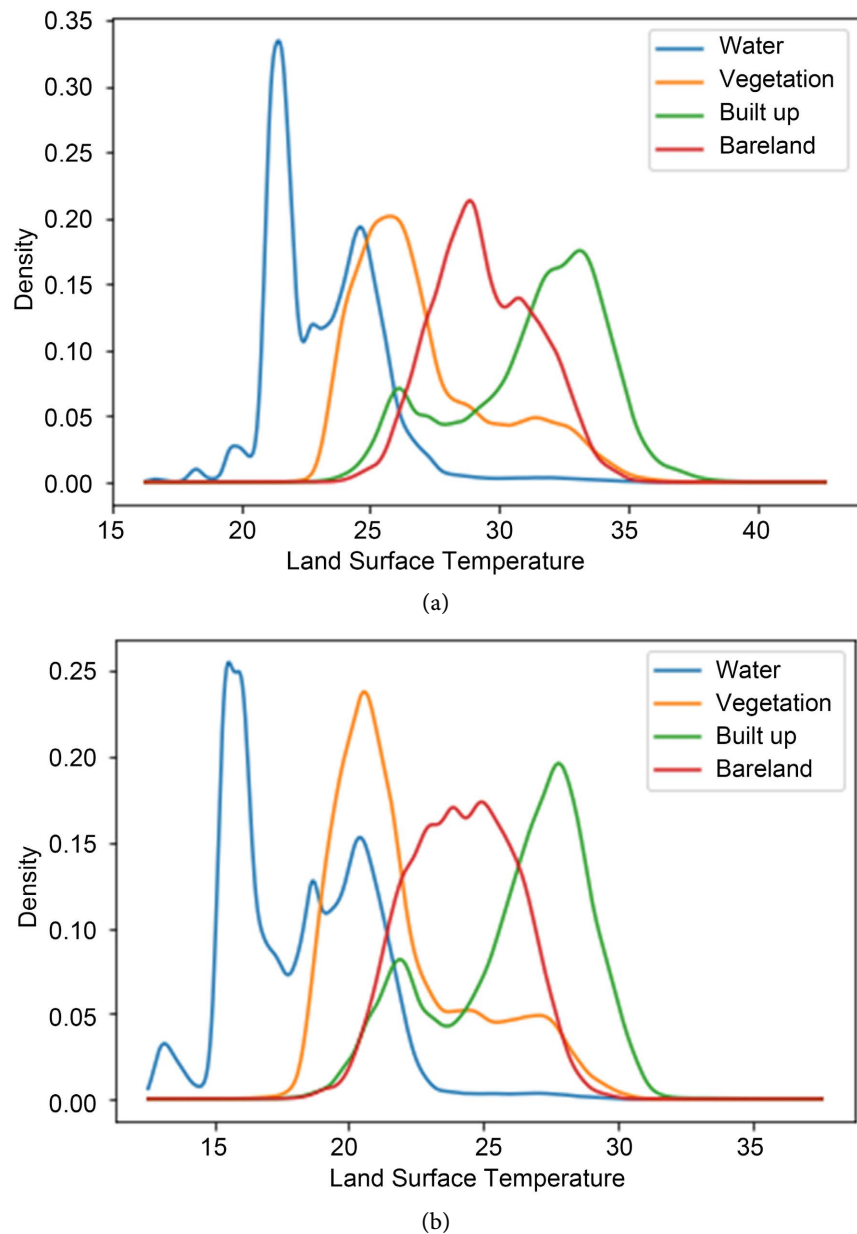


Figure 12. LST map for Orleans.

### 3.3. Urban Forestry Integration in Land Surface Temperature

A thorough analysis of the results of the three study areas depicts that green areas or forest spaces have a negative LST relationship, thus less LST recorded in most of the green that still recorded reduced LST during the lockdown. By this, it is also revealed that land cover classes that have higher LST values have shown the lowest NDVI values. This is because the surface radiant temperature is negatively correlated with NDVI for all the land use cover types. As a result, the highest NDVI value and the lowest LST value are observed in land cover types with vegetation, forests or urban green spaces. Aside from the regulatory control of human activities, natural mitigative measures such as urban greening could be adopted to reduce the impact of high LST especially in urban areas. In this regard, dense tree planting is considered as one of the strategies to mitigate the urban heat island effect, which is the phenomenon of urban areas being warmer than rural areas due to the built environment, human activities, and lack of vegetation. As the LST is a key indicator of the urban heat island effect which measures the temperature of the ground surface, dense tree reforestation can reduce the amount of direct sunlight or heat that reaches the ground to cause high surface temperatures especially in urban areas. In addition to trees providing shade to reduce the temperature of the ground surface, trees also provide an evaporative cooling effect which can help to reduce the temperature and improve air quality in urban areas. This shading effect can also significantly reduce the amount of heat absorbed by buildings and other structures. Agreeably, studies have agreed that urban areas with more tree cover tend to have lower LSTs compared to areas with less tree cover. For instance, [27] conducted a study on the impact of urban green spaces on urban heat islands in China where it was discovered that increasing the green space coverage in urban areas can significantly reduce the



**Figure 13.** Land surface temperature distribution for various land covers in Orleans within the study period: (a) March 2019 (before lockdown) (b) March 2020 (during lockdown).

surface temperature and air temperature, and that tree planting is the most effective way to mitigate the urban heat island effect. Dense greening is considered as one of the nature-based solutions to combat the effects from high concentrations of air pollutants that tend to absorb and re-emit heat back into the atmosphere. This is because trees remove Carbon-dioxide ( $\text{CO}_2$ ), one of the highly concentrated pollutants, through a process known as photosynthesis to reduce the heat-absorbing capacity of  $\text{CO}_2$  in the atmosphere. Also, trees transpire water through their leaves, which can help to cool the surrounding air. This process, known as evapotranspiration, can significantly reduce the air temperature and

LST in urban areas. The cooling effect of evapotranspiration is particularly effective in humid climates, where the air is already moist and can absorb more water vapor from the trees. Additionally, the water vapor released by trees can also improve air quality by reducing the concentration of pollutants and dust particles in the air. The results therefore depict the relationship between LST and greenspaces while highlighting how the latter can be adopted as a nature-based solution towards reducing high LST especially in urban areas. That is, urban planners and policymakers should consider these strategies when designing and managing urban areas, to improve the environment and quality of life for city dwellers.

### 3.4. COVID-19 Lockdown Impact on Land Surface Temperature

Population density, climate, and the intensity of commercial and industrial activities cause anthropogenic heat flux and diurnal and seasonal scale variabilities. Several factors such as differences in topography, meteorological conditions, anthropogenic emissions, and boundary layer dynamics firmly control the air quality and their impacts on the larger troposphere [2]. Anthropogenic activities such as industrialization, transportation, and energy demand have increased in urban areas which increases the albedo effect (low albedo). This leads to an increase in LST as well as air pollution, which could cause health risks associated with harmful pollutants and impose high social and economic social costs. However, it is observed that a reduction in anthropogenic activities and pollution due to COVID-19 induced lockdown was responsible for the decrease in LST for the three study areas. This is to say that COVID-19 lockdown offers an opportunity to examine the impacts of reduced heat emitted from surface transportation along with decreased air pollutants on LST and the UHI intensity [28]. For this reason, [2] opine that short-term lockdown restrictions can be implemented by the urban authorities which may be an essential and viable option as far as mitigating the effect of UHI and the declining air quality. Zambrano *et al.* (2016) therefore concluded that there is a significant relationship between contingency measures like lockdowns and improvement in air quality, environmental noise reduction, and clean beaches. As far as our environment is concerned, less human activities imply a healthy atmosphere in the absence of high land surface temperature.

## 4. Conclusion

Natural climatic changes, as well as several human activities such as industrialization, rapid urbanization, and other activities involving the combustion of fossil fuels, have a significant impact on the earth's near-surface temperature. The recurring mitigative strategy for this anomaly is centered on employing ecologically friendly alternative energy sources, reducing the amount of dangerous gases that are emitted into the atmosphere, and regulating certain unfavorable human activities. Although it has been linked to a few economic calamities, controlling human activities has nonetheless been observed as one of the strategies

that have a favorable impact on the environment, as evident during the COVID-19 pandemic detected in 2019, subsequently leading to a worldwide mandatory lockdown action. In fact, the COVID-19 pandemic and lockdown resulted in a temporary improvement of the near-surface temperature on a global level due to the significant decrease in transportation, industrial output and energy consumption. Considering that certain environmental changes were observed especially prior to and during the lockdown period, this study dwelled on this assertion to conduct research in this regard. Louisiana, being one of the South-central states, was the broad study area while focusing on East Baton Rouge, Orleans and Lafayette parishes as the three major study areas. The study employed a remote sensing methodology using Landsat 8 Thermal Infrared Sensor (TIRS) Level 2, Collection 2, Tier 2 data from the Google Earth Engine Catalog. The Land Surface Temperature (LST) product was gridded at a resolution of 30m, giving the data a spatial resolution of 100 m (or 328.08 feet). For the land cover classification, three Normalized Difference Indices including the Normalized Difference Vegetation Index (NDVI), Normalized Difference Water Index (NDWI) and Normalized Difference Built-Up Index (NDBI) were used to improve the accuracy of the image classifications using a random forest supervised classification algorithm. Following this, the results capture changes in the various land covers and their respective land surface temperatures as a result of the COVID-19 lockdown impact. In East Baton Rouge Parish, the land with the highest LST value decreased from approximately 44 degrees Celsius in 2019 to 38 degrees Celsius in 2020. Similarly, Lafayette also recorded a reduction in LST value from 42 degrees Celsius (2019) to 38 degrees (2020). Celsius approximately just as Orleans also recorded a reduction in LST values from 43 degrees Celsius (2019) to 38 degrees Celsius (2020) approximately. Notably, according to the images, most of the high LST values and an observed reduction were recorded from areas with concentrated built-up areas indicative of the influence of anthropogenic activities within those areas on LST. Concerning green spaces, the results reveal that there is a negative relationship between this land cover type and LST especially between the classes that had low LST values due to high NDVI values and vice versa. In addition to a reduction in human activities having favorable impacts on the environment, other nature-based solutions such as dense-planting are revealed as having a high potential for reducing LST and its associated effects. Even though this was not captured in the results, LST values have steadily been increasing since 2021 as a result of the return of normalized business and human activities. Hence, the study provided more insight into the fact that with fewer atmospheric pollutants and urban heat stress from anthropogenic activities, our environment can be restored to a healthier one. The COVID-19 outbreak and lockdown did, in fact, cause a major decline in energy use, transportation, and industrial activity, which temporarily improved the near-surface temperature on a worldwide scale. Hence, the study gave us more information about how to make our environment healthier by reducing anthropogenic air pollutants and urban heat stress.

## Acknowledgements

The authors would like to acknowledge the United States Department of Education's Higher Education Emergency Relief Fund (HEERF) and the Office of Sponsored Programs for providing financial support for the execution of this Research Project. Our earnest appreciation also goes to Professor Yaw A. Twumasi who doubled as a co-author and supervisor, to provide valuable input for the effective completion of this research paper. Also, the efforts of Ms. Matilda Anokye and her immense contributions to this paper are highly appreciated. Finally, the authors would like to acknowledge the United States Department of Agriculture (USDA) National Institute of Food and Agriculture (NIFA) McIntire Stennis Forestry Research Program funded project with award number NI22MSCFRXXXG077. Project title: Enhancing Graduate Education and Research Productivity in Urban Forestry and Natural Resource Management.

## Conflicts of Interest

The authors declare no conflicts of interest regarding the publication of this paper.

## References

- [1] Akorede, M.F., Hizam, H. and Aris, Z.K. (2012) Mitigating the Anthropogenic Global Warming in the Electric Power Industry. *Renewable and Sustainable Energy Reviews*, **16**, 2747-2761. <https://doi.org/10.1016/j.rser.2012.02.037>
- [2] Jallu, S.B., Shaik, R.U., Srivastav, R. and Pignatta, G. (2022) Assessing the Effect of COVID-19 Lockdown on Surface Urban Heat Island for Different Land Use/Cover Types Using Remote Sensing. *Energy Nexus*, **5**, Article ID: 100056. <https://doi.org/10.1016/j.nexus.2022.100056>
- [3] Shaftel, H., Callery, S. and Bailey, R.J. (2022) The Causes of Climate Change: Human Activities Are Driving the Global Warming Trend Observed since the Mid-20th Century. NASA—Global Climate Change: Vital Signs of the Planet. [https://climate.nasa.gov/causes/#otp\\_the\\_role\\_of\\_humans](https://climate.nasa.gov/causes/#otp_the_role_of_humans)
- [4] Levy, P.P. (2022) Earth Observatory: Land Surface Temperature. National Aeronautics and Space Administration. [https://earthobservatory.nasa.gov/global-maps/MOD\\_LSTD\\_M](https://earthobservatory.nasa.gov/global-maps/MOD_LSTD_M)
- [5] United States Environmental Protection Agency (2022) Report on the Environment. <https://www.epa.gov/report-environment/>
- [6] Ibrahim, I., Samah, A.A. and Noor, R.F. (2016) The Land Surface Temperature Impact to Land Cover Types. *The International Archives of the Photogrammetry, Remote Sensing and Spatial Information Sciences*, **XLI-B3**, 871-876. <https://doi.org/10.5194/isprs-archives-XLI-B3-871-2016>
- [7] Sarker, T. (2020) Role of Climatic and Non-Climatic Factors on Land Use and Land Cover Change in the Arctic: A Comparative Analysis of Vorkuta and Salekhard. George Washington Libraries. <https://scholarspace.library.gwu.edu/etd/6969z1516>
- [8] Twumasi, Y.A., Merem, E.C., Namwamba, J.B., Mwakimi, O.S., Ayala-Silva, T., Frimpong, D.B., Petja, B.M., *et al.* (2021) Estimation of Land Surface Temperature from Landsat-8 OLI Thermal Infrared Satellite Data. A Comparative Analysis of Two Cities in Ghana. *Advances in Remote Sensing*, **10**, 131-149.

- <https://doi.org/10.4236/ars.2021.104009>
- [9] Lindsey, R. (2021) Climate Change: Global Sea Level. <https://www.climate.gov/news-features/understanding-climate/climate-change-global-sea-level>
- [10] IPCC: Intergovernmental Panel on Climate Change (2019) IPCC Special Report on the Ocean and Cryosphere in a Changing Climate. [https://www.ipcc.ch/site/assets/uploads/sites/3/2019/12/02\\_SROCC\\_FM\\_FINAL.pdf](https://www.ipcc.ch/site/assets/uploads/sites/3/2019/12/02_SROCC_FM_FINAL.pdf)
- [11] Teufel, B., Sushama, L., Poitras, V., Dukhan, T., Bélair, S., Miranda-Moreno, L., Bitsuamlak, G., *et al.* (2021) Impact of COVID-19-Related Traffic Slowdown on Urban Heat Characteristics. *Atmosphere*, **12**, Article 243. <https://doi.org/10.3390/atmos12020243>
- [12] USAFacts (2022) Climate in East Baton Rouge Parish, Louisiana. <https://usafacts.org/issues/climate/state/louisiana/county/east-baton-rouge-parish>
- [13] Shailendra, J.K. and Taylor, R. (2018) Remote Sensing of Water Resources, Disasters, and Urban Studies. CRC Press, Boca Raton.
- [14] Jothimani, M., Gunalan, J. and Abel, R.D. (2021) Study the Relationship between LULC, LST, NDVI, NDWI and NDBI in Greater Arba Minch Area, Rift Valley, Ethiopia. *Atlantis Highlights in Computer Sciences*, **4**, 183-193. <https://doi.org/10.2991/ahis.k.210913.023>
- [15] Ardoin, K. (2022) Louisiana Facts—Compiled by Kyle Ardoin: Secretary of State. <https://www.sos.la.gov/HistoricalResources/PublishedDocuments/LouisianaFactsBooklet.pdf>
- [16] United States Census Bureau (2021) QuicFacts—East Baton Rouge Parish, Louisiana. <https://www.census.gov/quickfacts/eastbatonrougeparishlouisiana>
- [17] Abdollahi, K., Ning, Z., Legiandenyi, T. and Khanal, P. (2012) Urban Forest Ecosystem Structure, Function and Value—Baton Rouge, Louisiana. <https://doi.org/10.13140/RG.2.2.31065.36967>
- [18] Peters, E. (2022) What Type Of Climate Does Baton Rouge Have? <https://partyshopmaine.com/baton-rouge/what-type-of-climate-does-baton-rouge-have/>
- [19] Frimpong, D.B., Twumasi, Y.A., Ning, Z.H., Asare-Ansah, A.B., Anokye, M., Loh, P.M., Namwamba, J., *et al.* (2022) Assessing the Impact of Land Use and Land Cover Change on Air Quality in East Baton Rouge—Louisiana Using Earth Observation Techniques. *Advances in Remote Sensing*, **11**, 106-119. <https://doi.org/10.4236/ars.2022.113007>
- [20] Publications, T. (2022) Lafayette: A Place to Do Business. <https://townsquarepublications.com/major-industries-in-lafayette-la/>
- [21] Gitelson, A.A., Kaufman, Y.J. and Merzlyak, Y.J. (2003) Use of a Green Channel in Remote Sensing of Global Vegetation from EOS-MODIS. *Remote Sensing of Environment*, **58**, 289-298. [https://doi.org/10.1016/S0034-4257\(96\)00072-7](https://doi.org/10.1016/S0034-4257(96)00072-7)
- [22] Gao, B.C. (1996) A Normalized Difference Water Index for Remote Sensing of Vegetation Liquid Water from Space. *Remote Sensing of Environment*, **58**, 257-266. [https://doi.org/10.1016/S0034-4257\(96\)00067-3](https://doi.org/10.1016/S0034-4257(96)00067-3)
- [23] Zha, Y., Gao, J. and Ni, S. (2003) Use of Normalized Difference Built-Up Index in Automatically Mapping Urban Areas from TM Imagery. *International Journal of Remote Sensing*, **24**, 583-594. <https://doi.org/10.1080/01431160304987>
- [24] Jovanovska, U.A. (2016) Algorithm for Automated Mapping of Land Surface Temper-

- 
- ature Using LANDSAT 8 Satellite Data. *Journal of Sensors*, **2016**, Article ID: 1480307. <https://doi.org/10.1155/2016/1480307>
- [25] Modest, M.F. (2013) Radiative Heat Transfer. Academic Press, Cambridge. <https://doi.org/10.1016/B978-0-12-386944-9.50023-6>
- [26] Ziaul, S. and Pal, S. (2017) Detection of Land Use and Land Cover Change and Land Surface Temperature in English Bazar Urban Centre. *The Egyptian Journal of Remote Sensing and Space Sciences*, **20**, 125-145. <https://doi.org/10.1016/j.ejrs.2016.11.003>
- [27] Tong, Z., Yu, Y. and Wang, Y.X. (2022) Study on the Impact of Urban Green Space on Urban Heat Island Effect in Beijing-Tianjin-Hebei Region, China. *Academic Journal of Humanities & Social Sciences*, **5**, 4-6.
- [28] Parida, B.R., Bar, S., Kaskaoutis, D., Pandey, A.C., Polade, S.D. and Goaswami, S. (2021) Impact of COVID-19 Induced Lockdown on Land Surface Temperature, Aerosol, and Urban Heat in Europe and North America. *Sustainable Cities and Society*, **75**, Article ID: 103336. <https://doi.org/10.1016/j.scs.2021.103336>